

INTERNATIONAL SOCIETY FOR SOIL MECHANICS AND GEOTECHNICAL ENGINEERING



This paper was downloaded from the Online Library of the International Society for Soil Mechanics and Geotechnical Engineering (ISSMGE). The library is available here:

<https://www.issmge.org/publications/online-library>

This is an open-access database that archives thousands of papers published under the Auspices of the ISSMGE and maintained by the Innovation and Development Committee of ISSMGE.

The paper was published in the proceedings of the 7th International Conference on Earthquake Geotechnical Engineering and was edited by Francesco Silvestri, Nicola Moraci and Susanna Antonielli. The conference was held in Rome, Italy, 17 - 20 June 2019.

Numerical simulations of grid form deep mixing walls with non-liquefying sand layer

K. Kaneda

Takenaka R&D Institute, Inzai, Chiba, Japan

M. Imai & S. Tsukuni

Takenaka Civil Engineering & Construction Co., Ltd., Inzai, Chiba, Japan

ABSTRACT: Grid-form deep mixing walls are constructed using grid-form modified soil with cement surrounding the liquefiable sand to prevent liquefaction by suppressing the shear deformation caused by earthquakes. However, when the grid-form interval is large, it is possible that liquefaction occurs because the shear deformation of the liquefiable sand is not suppressed. On the other hand, it is found that liquefaction does not occur when a non-liquefiable sand layer is provided above the liquefiable sand (Ishihara, 1985). Numerical simulations were performed to investigate the effect of the non-liquefiable sand layer placed above the liquefiable sand layer. The simulation results show that as the non-liquefiable sand layer becomes thicker, the settlement within the grid-form deep mixing wall at the ground surface becomes smaller.

1 INTRODUCTION

Grid-form deep mixing walls, shown in Figure 1, are constructed using grid-form modified soil with cement surrounding the liquefiable sand to prevent liquefaction by suppressing the shear deformation during an earthquake. This method was proven effective during the Hyogoken Nanbu earthquake (1995) and the Great East Japan earthquake (2011). Figure 2 shows the liquefaction prevention mechanism of the grid-form deep mixing wall. By surrounding the liquefied ground with the improved wall, the shearing deformation of the ground during an earthquake can be reduced, thus preventing liquefaction. However, it may be noted that liquefaction may occur when the grid-form interval is large because the shear deformation of the liquefiable sand is not adequately suppressed in this case. Previous disaster investigations have revealed that when a non-liquefiable sand layer exists above a liquefaction layer, the liquefaction resistance increases with the thickness of the non-liquefiable sand layer. (Ishihara, 1985) Another research used a centrifuge model test to investigate the effect of a non-liquefiable sand layer above liquefiable sand during an earthquake. (Kaneda and Imai (2017)) Can the presence of the non-liquefiable sand layer above the liquefiable sand widen the grid-form interval? In this study, we investigate the influence of the difference in the grid-form intervals in liquefiable sand when a non-liquefiable sand layer is present above the liquefiable sand using numerical simulations. The two-phase (soil and water) dynamic numerical analysis code used is MuDIAN developed by Takenaka Corporation with SYS Cam-clay model. A series of dynamic analyses was performed with various grid-form intervals, various densities of liquefiable sand, and various thicknesses of the liquefied layers.

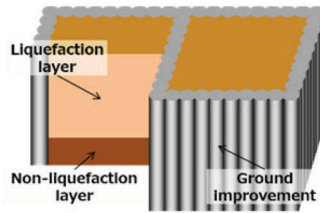


Figure 1. Structure of grid-form deep mixing walls.

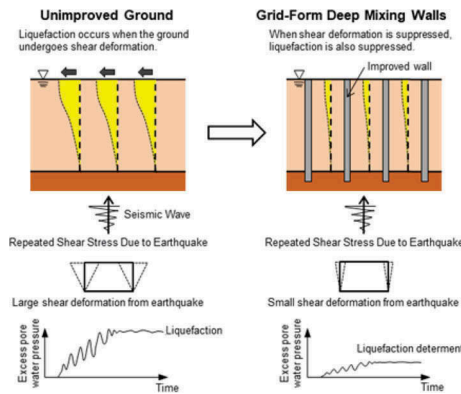


Figure 2. Liquefaction prevention mechanism by grid-form deep mixing walls.

2 ANALYTICAL CONDITIONS

Figure 3 shows an example of 3D numerical meshes for the case where a 3-m-thick non-liquefiable sand layer is present. The half-section of the soil is depicted, assuming symmetric conditions; the width of the grid-form deep mixing walls was 1 m. The foundation soil was set at the bottom to a depth of 5 m, and 10 m of liquefiable sand was set over it to form the first of the two phases. The non-liquefiable sand layer assumed as the second phase was set above the liquefiable sand. Table 1 shows the numerical simulation cases. The grid intervals were 6, 8, 10, 12, 14, and 16 m, and the depths of the non-liquefiable sand layers were 0, 1, 2, 3, 4, and 5 m in the finite element model. The side boundary condition was adopted as the repeated boundary in the dynamic analysis. Figure 4 shows the input JR Takatori EW wave in the Hyogoken Nanbu earthquake (maximum acceleration is 6.155 m/s) at the viscous bottom boundary. The simulation using this wave is case L, and the simulation using a wave with acceleration amplitude set at 50% is case S. As shown in Table 1, the simulations of both case L and S were performed without treatment (no grid-form deep mixing wall) at an interval of 10 m. The simulations of case L were performed with intervals of 6 and 8 m, and the

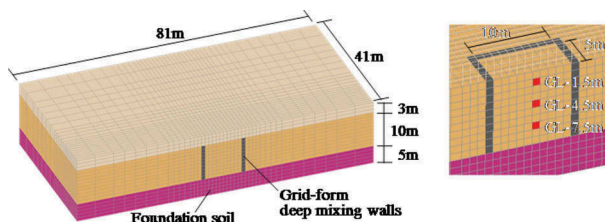


Figure 3. Numerical mesh (non-liquefiable sand layer: 3 m).

Table 1. Numerical cases.

		non-liquefying sand layer						
			0m	1m	2m	3m	4m	5m
I n t e r v a l	none	L/H	0-0	0-1	0-2	0-3	0-4	0-5
	6m	0.6	6-0	6-1	6-2	6-3	6-4	6-5
	8m	0.8	8-0	8-1	8-2	8-3	8-4	8-5
	10m	1.0	10-0	10-1	10-2	10-3	10-4	10-5
	12m	1.2	12-0	12-1	12-2	12-3	12-4	12-5
	14m	1.4	14-0	14-1	14-2	14-3	14-4	14-5
	16m	1.6	16-0	16-1	16-2	16-3	16-4	16-5
		Case S and Case L						
		Case L						
		Case S						

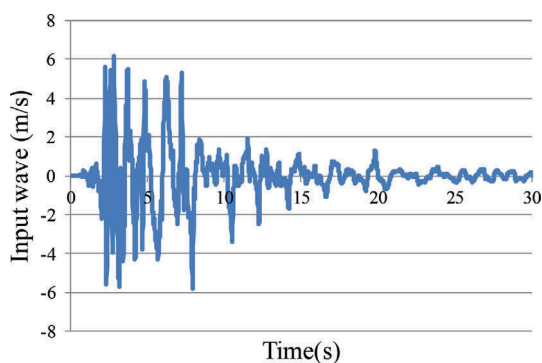


Figure 4. Input JR Takatori EW wave in the Hyogoken Nanbu earthquake (maximum acceleration is 6.155 m/s).

Table 2. Material parameters

<Elasto-plastic parameters>	Foundation soil	liquefying soil	Non-liquefying soil
Compression index λ	0.05	0.05	0.05
Swelling index κ	0.02	0.002	0.01
Critical state constant M	1.4	0.6	1.4
NCL intercept N (at $p' = 98$ kPa)	1.79	1.79	1.79
Poisson's ratio ν	0.1	0.1	0.3
<Evolution parameters>			
Degradation parameter of overconsolidated state m	0.3	0.3	0.05
Degradation parameter of structure a	2.2	2.2	2.2
Degradation parameter of structures b and c	1.0	1.0	1.0
Evolution parameter b_r	2.5	3.0	2.5
Limit of rotation m_b	0.5	1.0	0.5
<Initial conditions>			
Overconsolidation ratio R_0		3.75×10^{-2}	
Degree of anisotropy ζ_0	1.0	0.6	1.0
Coefficient of lateral pressure K_0	1.0	0.6	1.0
Degree of structure R^*_0	1.0	0.2	1.0
Density ρ_s (g/cm ³)		2.656	
Permeability k (m/s)	1.0×10^{-5}	1.0×10^{-5}	-

Treated soil

Elastic modulus E (kPa)	7.0×10^5
Poisson's ratio ν	0.3
Density ρ (t/m ³)	2.65
Permeability k (m/sec)	1.0×10^{-10}

simulations of case S were performed with intervals of 12, 14, and 16 m. The material parameters are shown in Table 2. These are the typical sand parameters of the SYS Cam clay model (Asaoka et al., 2002). The software used is MuDIAN (Shiomi et al., 1993) developed by Takenaka Corporation.

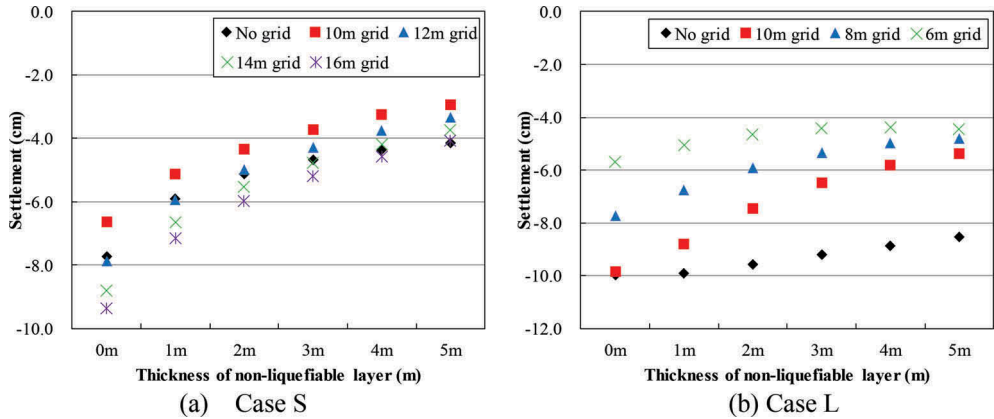
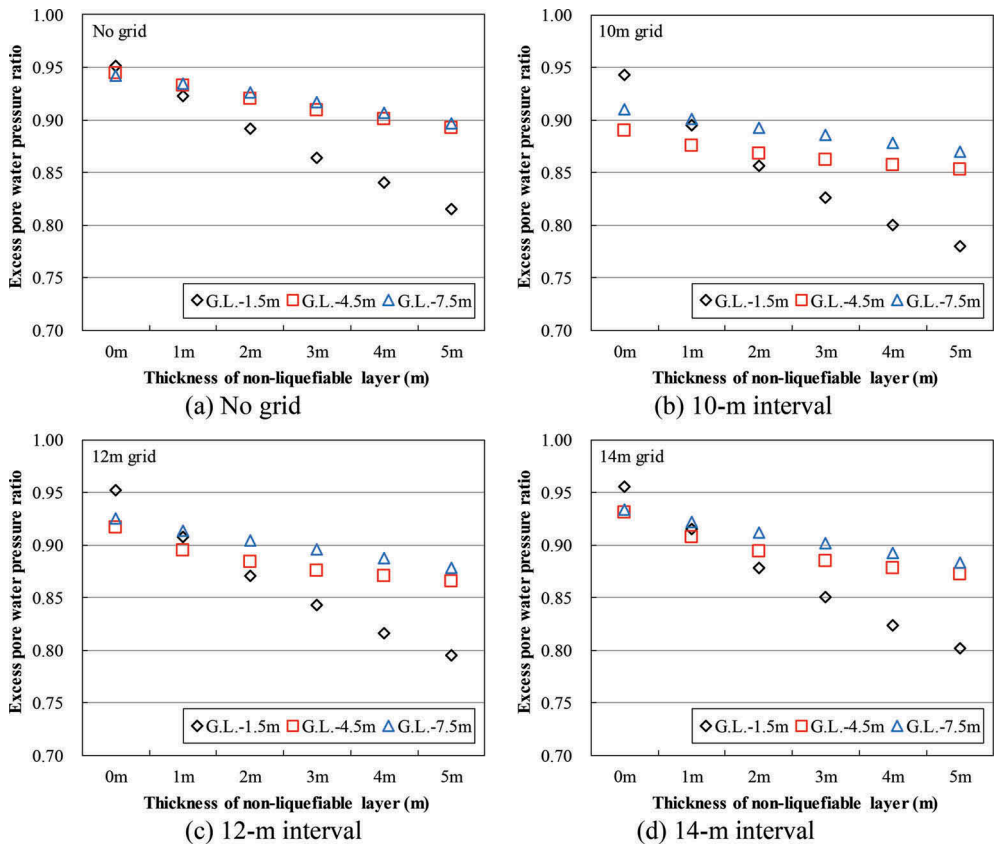


Figure 5. Relationship between the final settlement of the center of the grid-form deep mixing wall and thickness of the non-liquefiable sand layer.



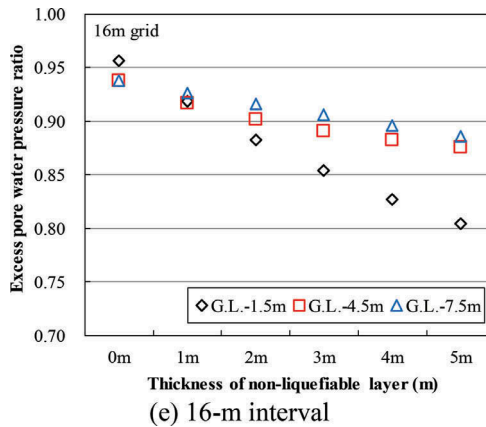


Figure 6. Relationship between excess pore water pressure ratio and thickness of the non-liquefiable sand layer.

3 ANALYSIS RESULTS AND DISCUSSION

Figure 5 shows the relationship between the final settlement of the center of the grid-form deep mixing wall and the non-liquefiable sand layer for the case S (a) and L (b). After the occurrence of the earthquake, consolidation analysis was performed until excess pore pressure dissipated. As the non-liquefiable sand layer became thicker, the amount of settlement decreased in both cases. In the case S with interval of 16 m, it can be seen that the final settlement was suppressed to nearly 4 cm or less when the depth of the non-liquefiable sand layer was 5 m. On the other hand, in case L, the amount of settlement increased because of the increase in seismic motion; moreover, the amount of settlement did not reduce significantly even when the thickness of the non-liquefiable sand layer increased in the untreated case. The amount of settlement for the interval of 6 m did not differ greatly between the non-liquefying sand layer thicknesses of 0 m and 5 m. However, it was reduced by approximately 5 cm for the interval of 10 m. The thicker the non-liquefying sand layer and the wider the interval of the grid-form deep mixing walls, the smaller is the amount of settlement. This is considered as the effect of the increasing confining pressure exerted by the thicker non-liquefiable sand layer on the liquefying layer. Figure 6 shows the relationship between excess pore water pressure ratio and thickness of the non-liquefiable sand layer for case S with no grid (a) and with grid intervals of 10 (b), 12 (c), 14 (d), and 16 m (e). The symbols black diamond, red square, and blue triangle indicate the depths corresponding to GL-1.5 m, GL-4.5 m, and GL-7.5 m at the center of the grid-form deep mixing walls, respectively, as shown in Figure 3. When the thickness of the non-liquefiable sand layer is 0 m, each value of the excess pore water pressure ratio is over 0.9 and liquefaction is observed. As the non-liquefying sand layer becomes thicker, the excess pore water pressure ratio decreases. Especially, this decrease is larger near the ground surface. The confining pressure on the liquefying layer, which increases as the non-liquefying sand layer becomes thicker, is considered the reason for this decrease in the excess pore water pressure ratio; consequently, the liquefaction resistance increases. In this research, the excess pore water pressure ratio was defined as the rate of reduction of the mean effective stress.

Figure 7 shows the distribution of the settlement for the grid interval of 10 m in case L for each thickness of the non-liquefiable sand layer. Figure 7 (a) shows the surface settlement, (b) shows the settlement of the upper surface of the liquefiable sand layer (immediately below the non-liquefiable sand layer), and (c) is the differences between (a) surface settlement and (b) settlement of the upper surface of the liquefiable sand layer, which

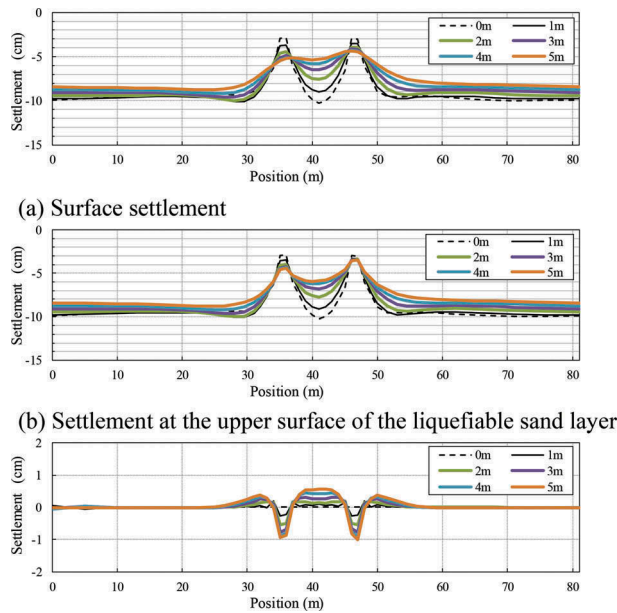


Figure 7. Distributions of settlement for the grid interval of 10 m in case L.

changes with the thickness of the non-liquefiable sand layer. From Figure 7 (a), as the non-liquefiable sand layer becomes thicker, the settlement within the grid-form deep mixing wall at the ground surface becomes smaller, but the amount of settlement of the grid-form deep mixing wall increases. The difference between the settlement at the surface of the grid-form deep mixing wall and that within it is relatively small. As the non-liquefiable sand layer becomes thicker, the settlement at the upper surface of the liquefiable sand layer in the grid-form deep mixing wall becomes smaller. However, it is larger than the surface settlement in (a). On the other hand, the settlement of the grid-form deep mixing wall is small, approximately 2 cm, regardless of the thickness of the non-liquefiable sand layer. From (c), as the non-liquefiable sand layer becomes thicker, the displacement within and around the grid-form deep mixing wall becomes positive, which indicates that the settlement of the liquefiable layer is larger than that of the ground surface. In other words, when the non-liquefiable sand layer in the grid-form deep mixing wall subsides, it is considered that the soil at the ground above the small settlement on the wall is drawn into the wall. The thicker the non-liquefiable sand layer, the larger is the amount of soil that is drawn. It is considered that the unevenness of the ground surface becomes small owing to the relaxation of the settlement generated in the liquefiable layer by the non-liquefiable sand layer.

4 CONCLUSION

The objective of this research was to understand the effect of grid-form deep mixing walls on the generation of excess pore water pressure and the surface morphology when a non-liquefaction layer is present on top of the liquefaction layer. Numerical simulations were performed to investigate the effect of the non-liquefiable sand layer placed above the liquefiable sand layer. The numerical software MuDIAN was used along with a SYS Cam clay model. A relatively large acceleration wave and a wave of half the acceleration were considered in these simulations. The following conclusions were obtained from the simulations:

1. As the non-liquefiable sand layer became thicker, the settlement within the grid-form deep mixing wall at the ground surface became smaller. It became clear that liquefaction could be suppressed by introducing a non-liquefying sand layer.
2. The effect of the non-liquefying sand layer was investigated after the settlement. Settlement occurred inside the grid-form deep mixing wall, whereas there was hardly any settlement on the grid-form deep mixing wall, which may cause unevenness. As the non-liquefiable sand layer became thicker, the unevenness of the ground surface reduced. This was because the settlement generated in the liquefying layer by the non-liquefying sand layer was relaxed.

REFERENCES

- Asaoka, A., Noda, T., Yamada, T., Kaneda, K. and Nakano, M. 2002. An elasto-plastic description of two distinct volume change mechanisms of soils, *Soils and Foundations*, 42(5),47-57.
- Ishihara, K. 1985. Stability of natural deposits during earthquake, *11th Inter. Conf. on Soil Mech and Foundation Eng.*, Vol. 1, pp. 321-376.
- Shiomi, T., Shigeno, Y. and Zienkiewicz, O. C. 1993. Numerical prediction for model No.1, Verification of Numerical Procedures for the Analysis of Soil Liquefaction Problems (eds. Arulanandan and Scott), Balkema, pp. 213-219.
- Kaneda, K. and Imai, M. 2017. Preventing liquefaction by using grid-form deep mixing walls on a liquefiable soil layer below a nonliquefiable layer, Proc. of the 19th Int. Conf.on Soil Mechanics and Geotechnical Engineering, Seoul, 2017.